Systems/Circuits

Local Field Potentials in the Gustatory Cortex Carry Taste Information

Rodrigo Pavão,[1] Caitlin E. Piette,[2] Vítor Lopes-dos-Santos,[1] Donald B. Katz,[2] and Adriano B.L. Tort[1]

[1]Brain Institute, Federal University of Rio Grande do Norte, RN 59056-450, Brazil and [2]Psychology Department and Volen Center for Complex Systems, Brandeis University, Waltham, Massachusetts 02453

It has been recently shown that local field potentials (LFPs) from the auditory and visual cortices carry information about sensory stimuli, but whether this is a universal property of sensory cortices remains to be determined. Moreover, little is known about the temporal dynamics of sensory information contained in LFPs following stimulus onset. Here we investigated the time course of the amount of stimulus information in LFPs and spikes from the gustatory cortex of awake rats subjected to tastants and water delivery on the tongue. We found that the phase and amplitude of multiple LFP frequencies carry information about stimuli, which have specific time courses after stimulus delivery. The information carried by LFP phase and amplitude was independent within frequency bands, since the joint information exhibited neither synergy nor redundancy. Tastant information in LFPs was also independent and had a different time course from the information carried by spikes. These findings support the hypothesis that the brain uses different frequency channels to dynamically code for multiple features of a stimulus.

Introduction

It has been previously shown that rats can discriminate tastes (Scalera, 2000; Sadacca et al., 2012), and that neurons from the nucleus of the solitary tract (Lemon and Smith, 2006) and gustatory cortex (GC; Yamamoto et al., 1989; Katz et al., 2001; Samuelsen et al., 2012) are modulated by taste identity. Tastants delivered on the tongue also lead to evoked potentials and changes in the oscillatory activity of GC local field potentials (LFPs; Tort et al., 2010). However, it remains to be determined whether GC LFP responses are unspecific for taste stimuli, or if they depend on tastant identity. This last possibility is plausible, since LFPs reflect an integration of synaptic inputs that may complement spike coding (Logothetis, 2002). In fact, it was recently shown that LFPs from visual and auditory cortices carry information about moving images and natural sounds, respectively (Belitski et al., 2008, 2010; Montemurro et al., 2008; Kayser et al., 2009). Moreover, the information carried by different frequency bands may be independent (Belitski et al., 2008, 2010), and, further, in the auditory cortex the information contained in LFP amplitude is not redundant with the information contained in LFP phase (Kayser et al., 2009). Whether these are general properties of all sensory cortices remains to be shown. In addition, the time course of the amount of information in LFPs following stimulus onset has not been characterized; it is currently unknown, for example, if the temporal dynamics of LFP information follows that of spike responses.

In the present work, we recorded LFPs and spiking activity from the GC of awake rats subjected to delivery of small aliquots of sucrose, sodium chloride, citric acid, or quinine (exemplars of sweet, salty, sour, and bitter, respectively), interleaved with water rinse, on the tongue (Fig. 1). Using an information theoretic approach, we measured the amount of mutual information (MI) between taste identity and the phase and amplitude of frequency components of GC LFPs using a 1 ms time resolution. This approach allowed us to investigate the time course of information content, from tastant delivery and initial neuronal responses until signal stabilization, seconds after. We found that both the phase and amplitude of LFPs carry information about taste, which was independent from one another and also independent from the information contained in spike counts. The information carried by LFPs and spikes had different time courses following tastant delivery, and, moreover, different frequency bands exhibited different information dynamics. Our results suggest that spike counts and the amplitude and phase of field responses in GC have complementary roles in taste coding.

Materials and Methods

Subjects. We used female Long–Evans rats ($n = 21$; 275–300 g at time of surgery), maintained on a 12 h light/dark cycle; all experiments were performed during the light period of the cycle. Chow and water were available *ad libitum*.

Surgery. Anesthesia was induced and maintained using intraperitoneal injections of a mixture of ketamine, xylazine, and acepromazine (100, 10, and 10 mg/kg, respectively, for induction; 1/3 induction dose every 1.25 h for maintenance). Animals were placed on a stereotaxic frame, had the scalp excised, and holes were bored in the skull for ground screws, elec-

Received March 5, 2014; revised April 30, 2014; accepted May 21, 2014.

Author contributions: R.P., C.E.P., V.L.-d.S., D.B.K., and A.B.L.T. designed research; R.P. and C.E.P. performed research; V.L.-d.S. contributed unpublished reagents/analytic tools; R.P. analyzed data; R.P. and A.B.L.T. wrote the paper.

This work is supported by National Institutes of Health Grant DC006666, Conselho Nacional de Desenvolvimento Científico e Tecnológico, Coordenação de Aperfeiçoamento de Pessoal de Nível Superior, and Fundação de Apoio à Pesquisa do Estado do Rio Grande do Norte.

The authors declare no competing financial interests.

Correspondence should be addressed to Dr. Adriano B. L. Tort, Brain Institute, Federal University of Rio Grande do Norte, Rua Nascimento de Castro, 2155, Natal, RN 59056-450, Brazil. E-mail: tort@neuro.ufrn.br.

DOI:10.1523/JNEUROSCI.0908-14.2014

 0270-6474/14/348778-10$15.00/0

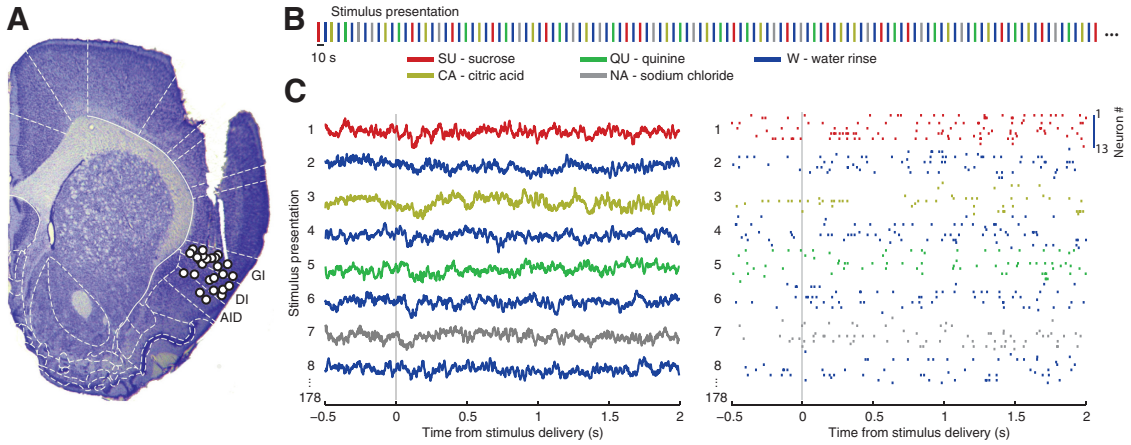

Figure 1. Experimental design. ***A***, Sample histology showing placement of electrode tips of the 21 rats included in the analysis. AID, agranular insular cortex (dorsal); DI, dysgranular insular cortex; GI, granular insular cortex. Adapted from Piette et al. (2012). ***B***, Stimulation protocol. Fluids were delivered through an IOC (session length: 30 min). Tastants (NA/SU/SA/QU) were presented randomly and interleaved with water delivery. The time between each fluid delivery was 10 s. ***C***, Example LFP signals (left) and spike rastergram (right) across trials. In this and other figures, time stamp 0 denotes onset of fluid delivery.

trode bundles, and guide cannulae. Bundles of 16 Formvar-coated, 25 μm nichrome wires were inserted 0.5 mm above the GC in both hemispheres [coordinates: anteroposterior (AP) 1.4 mm and mediolateral (ML) ±5 mm from bregma; dorsoventral (DV) − 4.5 mm from dura; (Fig. 1*A*)]. Guide cannulae were inserted into the basolateral amygdala (AP −3 mm and ML ±5.1 mm from bregma; DV −7.7 mm from skull) for another set of experiments (Piette et al., 2012); no infusion was done through the cannulae before or during the sessions analyzed in the present study. Once in position, electrode bundles were cemented to the skull with dental acrylic, along with two intraoral cannulae (IOCs), which were flexible plastic tubing inserted close to the tongue through the cheek and extending upward to the top of the skull. Rats were given 7 d to recover from surgery.

Fluid delivery. After beginning a regimen of mild water restriction (45 min per day, from 7 d following surgery), rats were habituated for several days to the test chamber and IOC delivery of water. The testing session was identical to adaptation sessions, but with 40 μl aliquots of the following (in M): 0.1 NaCl (NA), 0.1 sucrose (SU), 0.2 citric acid (CA), and 0.001 quinine-HCl (QU). Tastes were selected randomly without replacement, and taste deliveries were interleaved with a 40 μl aliquot of water; the time between each fluid delivery was 10 s. The testing session lasted ~30 min, including at least 20 trials of each tastant, and 80 trials of water (Fig. 1*B*).

Electrophysiology. For spiking activity, recordings were amplified, filtered at 300–8000 Hz, and digitized (Plexon). Single neurons of at least 3:1 signal-to-noise ratio were isolated on-line using an amplitude criterion in cooperation with a template algorithm (Nicolelis et al., 1997); off-line analysis confirmed and corrected on-line discriminations. Raw signals were also split off to a separate amplifier with filtering set for LFP recordings (bandpass 0.5–300 Hz) and from there to a computer, where they were digitized at 1000 Hz. One to 18 (7.1 ± 4.5) units and 2–16 (12.7 ± 4.1) LFP channels per rat were included in data analysis (Fig. 1*C*).

Data analysis. All analyses were done using built-in and custom routines written in MATLAB (MathWorks).

LFP filtering, and estimation of phase and amplitude. LFP signals were filtered with a linear finite impulse response filter using the *eegfilt* function from the EEGLAB Toolbox (Delorme and Makeig, 2004; http://sccn.ucsd.edu/eeglab/). The analytical representation of the signal based on the Hilbert transform (*hilbert* function from the Signal Processing Toolbox) was used to obtain the instantaneous amplitude and phase time series (Figs. 2*A*, 4*A*).

Evoked response and phase-reset index. The gustatory evoked potential response was obtained by averaging LFPs epochs triggered by stimulus delivery time. The averaging was done first over trials for each channel, and then over channels for each rat, and finally over rats. Fast components were removed by low-pass filtering the mean signal <30 Hz in Figure 5*B*. The phase-reset index was computed as previously described (Tort et al., 2010). For each instant of time, this metric assumes a value from 0 to 1, which corresponds to the level of phase consistency across trials; 1 means that the same phase occurred across trials for the corresponding time and 0 means no preferred phase across trials.

Spiking activity. Multiple isolated neurons (single units) were pooled into a single time series (pooled units). A continuous time series of firing rate was generated by convoluting spike times with a Gaussian ($\sigma = 25$ ms, so that 95% of the Gaussian of a single spike was included in spike time ± 50 ms). The same sampling rate of the LFP (1000 Hz) was used for the firing rate time series; the final time series was obtained by dividing by the number of neurons in the pool (Fig. 7*A*).

MI. The reduction of the uncertainty about a variable (in our case, tastant identity) due to the realization of another variable (e.g., LFP amplitude) is called MI. The entropy (H) measures the uncertainty of a random variable X:

$$H(X) = -\sum_x p(x) \times \log2(p(x)). \quad (1)$$

The joint entropy of a pair of random variables X and Y is given by the following:

$$H(X, Y) = -\sum_{x,y} p(x, y) \times \log2(p(x, y)). \quad (2)$$

The MI is computed as follows:

$$\mathrm{MI}(X, Y) = H(X) + H(Y) - H(X, Y), \quad (3)$$

which is equivalent to

$$\mathrm{MI}(X, Y) = \sum_{x,y} p(x, y) \times \log2(p(x, y)/p(x)p(y)). \quad (4)$$

In our study, X refers to the stimuli, and Y refers to values assumed by a neurophysiological variable (i.e., LFP amplitude, LFP phase or firing rate), which were binned into four equipopulated bins (quartiles; Kayser et al., 2009).

The MI estimated directly from the equations above, called naive MI, is biased due to the finite number of samples used to estimate the true distributions (Panzeri et al., 2007). To correct for finite sampling errors, we used a shuffling procedure associated with the Panzeri and Treves method (Panzeri and Treves, 1996; Panzeri et al., 2007), which was implemented in the toolbox described by Magri et al. (2009). Figures 2 and 4 show an overview of signal binning into quartile bins and MI estimation as a function of time around stimulus delivery; the same procedure was applied to pooled spike counts (Fig. 7). For the color-coded plots shown in Figures 3, *A* and *C*, and 5*A*, left, we bandpassed signals using 1 Hz windows centered at integer values (e.g., information in 5.5–6.5 Hz is represented by the 6 Hz y-tick); for the line plots on the right, we filtered

signals as indicated on the labels. For each rat, the information was calculated for each LFP channel separately and then averaged over channels. Except for Figure 5*C*, all results are presented as mean over animals (that is, $n = 21$ in all analyses).

Synergy analysis. The information between stimuli and two or more neurophysiological signals (e.g., LFP amplitude and LFP phase) allows evaluating the existence of synergy or redundancy among them. Synergy occurs when two or more variables evaluated together have higher MI than the sum of the MI associated to each variable separately. The level of synergy is defined by

$$\mathrm{Syn}(X; Y1, Y2) = \mathrm{MI}(X; Y1, Y2) - \mathrm{MI}(X, Y1) - \mathrm{MI}(X; Y2). \quad (5)$$

Synergy occurs if $\mathrm{Syn}(X;Y1,Y2) > 0$; otherwise, if $\mathrm{Syn}(X;Y1,Y2) < 0$, variables are said to be redundant. It should be noted that distributions with more categories or smaller sample sizes have larger bias in MI estimation. Because the joint distribution has more bins (in our case, $4 \times 4 = 16$ bins) than the marginal distributions (4 bins each) for the same sample size, in these analyses we applied an additional bias correction: for each channel, the mean prestimulus MI (from -3 to -1 s) was subtracted from each of the MI estimates on the right hand side of Equation 5. Similarly to the above equation, MI was obtained by the average over channels for each rat, while results (Figs. 6*B*, 7*E*) are presented as mean over rats ($n = 21$).

Finally, we performed an additional analysis of synergy/redundancy previously described by Schneidman et al. (2003). Briefly, the time series of LFP amplitude and phase were shuffled across trials of the same stimulus; this procedure thus breaks the dependence between phase and amplitude within trials but does not change the individual amount of information (since the marginal distribution is unchanged for each stimulus). We then compared the actual value of joint information in LFP phase and amplitude with the shuffled distribution of independent phase and amplitude ($n = 200$ surrogates). This analysis was performed for the time-frequency ranges associated with highest MI values.

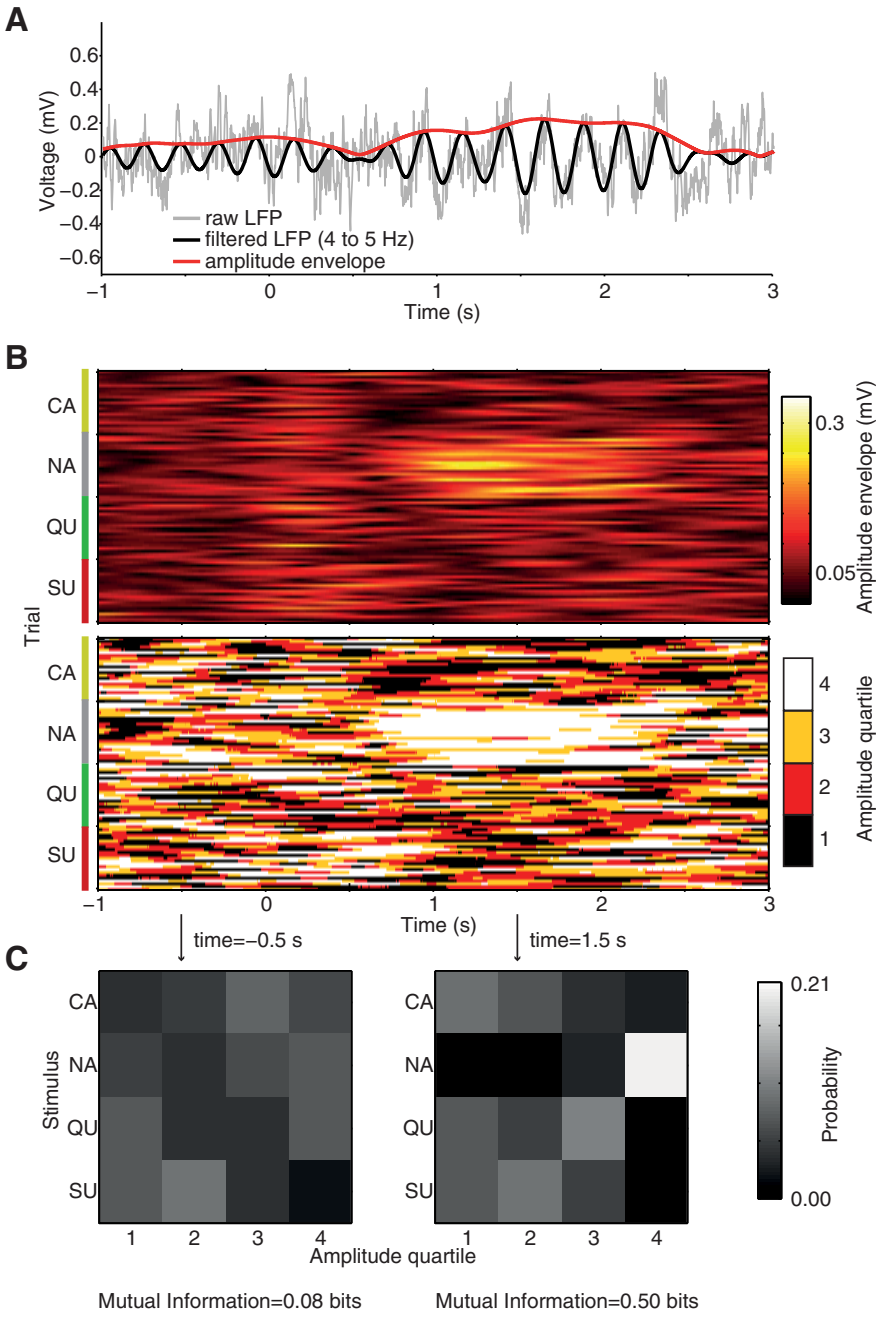

Figure 2. Estimating taste information in LFP amplitude. ***A***, Raw LFP (gray) and filtered signal (black) and its amplitude envelope (red) for an example trial. ***B***, Amplitude envelope of the filtered LFP signal as a function of time for all trials of each of the four tastants (top). Amplitude values binned into quartiles (bottom). ***C***, Two examples of joint probability distribution of stimuli and amplitude quartiles, which is used to compute the MI in each time bin. Since the probability of each tastant is the same (0.25), a uniform distribution indicates lack of MI between amplitude and stimuli.

Results

Taste information in GC LFP amplitude

We first investigated whether there is any taste specificity in the amplitude of different frequency components of LFP responses to taste stimuli. We computed the MI between stimuli and the amplitude of filtered LFPs following the procedure described in Figure 2, which allows obtaining MI estimates at a millisecond resolution (i.e., 1000 Hz sampling rate). Briefly, the LFP is filtered into the frequency band under study and the amplitude envelope of the filtered signal is obtained (Fig. 2*A*); for each time point, amplitude values across trials are binned into four quartiles (Fig. 2*B*); the MI is computed using the joint probability distribution between binned amplitude values and taste stimuli (Fig. 2*C*). We estimated the amount of stimulus information in LFP amplitude at every time step from 4 s before to 8 s after stimulus delivery (in the figures we focus on a shorter range where changes take place). In this work we evaluated two distributions separately: one composed by responses to the four tastants (CA, NA, QU, and SU), and another composed by the four tastants plus the responses to water (W). Figure 3, *A* and *C*, top, show the MI between tastants and LFP amplitude for multiple frequencies at different times around stimulus delivery. Before stimulus delivery (baseline), the sensory information contained in LFP amplitude was low for all analyzed frequencies. Interestingly, both the lowest (<10 Hz) and the highest (>100 Hz) part

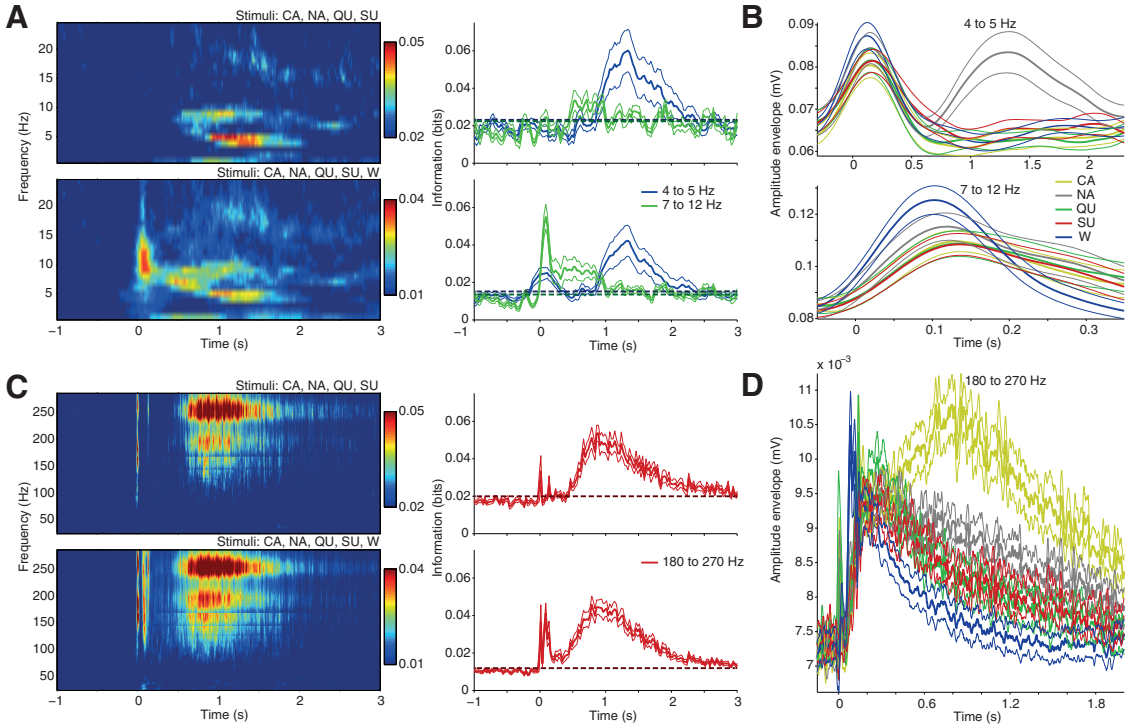

Figure 3. GC LFP amplitude carries information about tastants and water. ***A***, Top, left, MI between tastants and the amplitude of low LFP frequencies (1 Hz bins) as a function of time. Top, right, Time course of the amount of tastant information carried by the amplitude of 4–5 and 7–12 Hz frequency bands (mean ± SEM over rats). Dashed lines denote the upper limit of the 95% confidence interval of information values during baseline. Bottom shows similar analysis when also considering water as a stimulus. Note that 4–5 Hz has information about tastants in 1–2 s after fluid delivery, while 7–12 Hz carries information about water during the first second. ***B***, Mean amplitude envelope (±SEM) of 4–5 and 7–12 Hz filtered signals for each stimulus. Notice that NA is associated with large 4–5 Hz amplitude from 1 to 2 s, while water delivery leads to highest 7–12 Hz amplitude from 0 to 0.1 s. ***C***, Same as ***A***, but for high LFP frequencies (left) and analyzing further the 180–270 Hz frequency range (right). Notice that 180–270 Hz has information about tastants and water from 0.5 to 2 s. The information peaks at 0 and 0.13 s were deemed spurious and caused by artifacts from the opening and closing of fluid dispensers. ***D***, Same as ***B***, but for the 180–270 Hz frequency band; notice that W and CA induce the lowest and highest amplitude, respectively.

of the LFP frequency spectrum increased information about tastant identity following stimulus delivery. Information content started to increase from chance levels at ~0.5 s after stimulus delivery for the amplitude of higher frequency components (Fig. 3*C*, top right), while it was significantly above baseline ~0.8 s after stimulus delivery for the lower LFP frequencies (Fig. 3*A*, top right). Information returned to baseline levels at ~2 s post stimulus for all frequencies. Considering water (W) as a stimulus did not markedly change the dynamics of information content in the amplitude of high-frequency LFP components (Fig. 3*C*, bottom), but generated significant levels of information in the amplitude of 7–12 Hz LFP components from 0 to ~1 s after fluid delivery (Fig. 3*A*, bottom).

The time-frequency ranges of high information content reflect different taste-amplitude specificities. For example, the high tastant information observed in 4–5 Hz from 1 to 2 s indicates that amplitude values at this frequency and time period differ among tastants. Consistent with this, Figure 3*B*, top, shows that LFP responses following NA delivery have higher mean amplitude in this time-frequency range compared with other fluids. Similarly, the high level of information in the amplitude of 7–12 Hz from 0 to 1 s present only when water is taken into account (Fig. 3*A*, compare top and bottom) indicates that there is no amplitude specificity for the four tastants in this time-frequency range, and that the amplitude changes at 7–12 Hz should differ following water versus tastant delivery. Indeed, Figure 3*B*, bottom, shows that water induces an earlier increase in the amplitude of 7–12 Hz compared with other stimuli. Finally, the high taste-amplitude information in 180–270 Hz from 0.5 to 2 s is associated with different mean changes in amplitude at this range following the delivery of different tastants (Fig. 3*D*).

In all, our results show that GC LFP amplitude contains information about stimulus quality in specific frequencies and time epochs after stimulus delivery.

Taste information in GC LFP phase

We used a similar procedure as above to investigate whether there is taste specificity in the time-frequency representation of the LFP phase (Fig. 4). Figure 5*A*, top, shows that the phase of very slow LFP frequency components (<1.5 Hz) contains tastant information, which rises following stimulus delivery, peaks at ~800 ms afterward, and slowly decreases back to baseline levels 3 s post stimulus. In addition, the phase of 2–16 Hz LFP frequencies contained information about water in the first 500 ms post stimulus (Fig. 5*A*, bottom). The phase of higher frequency components (>25 Hz) exhibited no increase in information content after fluid delivery (except for the short time interval of opening and closing of fluid dispensers [not shown], which we deemed to be spurious as in Fig. 3*C*). And, similarly to the amplitude, tastant information in LFP phase was steadily low before stimulus delivery for all frequencies.

The existence of taste specificity in the instantaneous phase of slow GC LFP components suggests that gustatory evoked potentials (Tort et al., 2010) might be different among stimuli. We next investigated this possibility, and found that the negative peak of the evoked potential to water had shorter latency than to tastants (Fig. 5*B*); this earlier deflection accounts for the information in the phase of 2–16 Hz frequencies observed when water is also considered

a stimulus. This was further confirmed by the analysis of filtered signals and associated phase time series (Fig. 5*C*). These results show that the instantaneous phase of slow LFP frequency components carries tastant information.

Independent taste information in GC LFP phase and amplitude

We next analyzed the information content in the joint distribution of LFP phase and amplitude. In particular, we sought to determine whether the simultaneous evaluation of amplitude and phase would reveal synergistic or redundant information about tastants. Synergy occurs when the amount of information conveyed by the combined analysis of phase and amplitude is larger than the sum of the information conveyed by each signal evaluated individually. Redundancy is defined as the opposite of synergy, that is, when the joint distribution of phase and amplitude has less information than the sum of the information carried by each signal alone. If neither synergy nor redundancy occurs, the information carried by the individual signals is said to be independent. Figure 6*A* shows the time-frequency representation of taste information contained in the joint distribution of phase and amplitude. Notice that the time-frequency ranges associated with high values of information in the joint distribution correspond precisely to those observed in the marginal distributions (compare Figs. 3*A*,*C*, 5*A*). In particular, there was no new "informative" range of frequency and time in the combined analysis that was not present in the time-frequency representation of the information conveyed by either phase or amplitude considered alone.

We next investigated whether the information in LFP amplitude and phase for a same frequency range and time interval is redundant, independent, or synergistic. To that end, for each rat we averaged information values from informative time-frequency ranges for the marginal and joint distributions, as assessed by the time-frequency representation of information content for each case (that is, Figs. 3*A*,*C*, 5*A*, 6*A*). We then compared the amount of tastant information carried by the joint distribution of phase and amplitude with the sum of (individual) amplitude information and phase information (Fig. 6*B*). As shown in the two rightmost bars of Figure 6*B*, we found that the information about tastants in the joint distribution is approximately the same as the amplitude information plus the phase information. Given the absence of synergy or redundancy, these results show that the information conveyed by LFP amplitude and phase is independent.

The results above were confirmed by a trial-shuffling procedure that preserves stimulus identity (see Materials and Methods). This analysis keeps individual information values unchanged but breaks redundancy or synergy (Schneidman et al., 2003). Under this framework, we observed that the amount of taste information carried by actual joint distributions of amplitude and phase was not different from the information values obtained for shuffled joint distributions in which signals are independent by definition (data not shown).

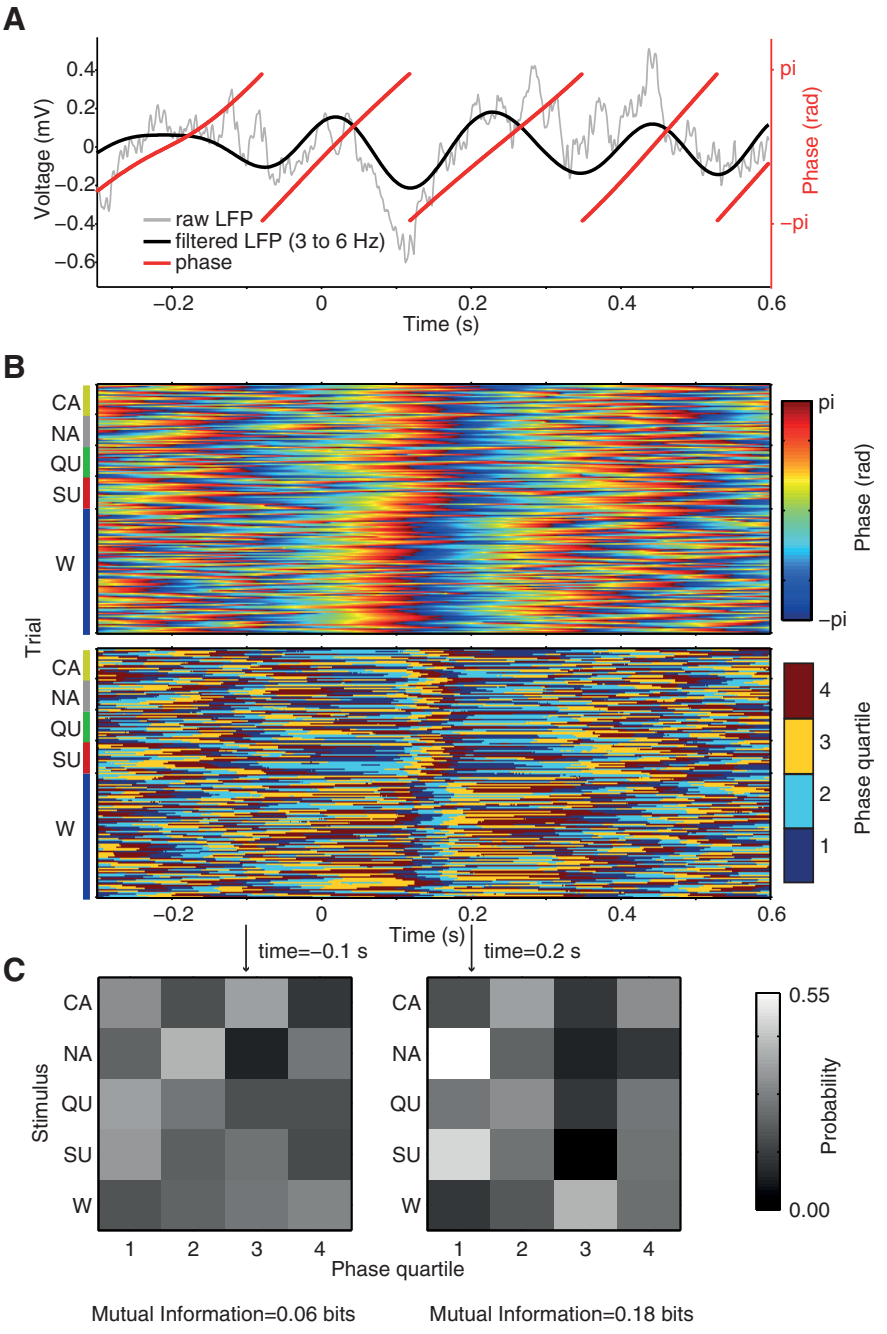

Figure 4. Estimating sensory information in LFP phase. ***A***, Raw LFP (gray) and filtered signal (black) and its phase time series (red) for an example trial. ***B***, Continuous and binned phase values as a function of time for the different tastants and water. ***C***, The MI is calculated from the joint probability distribution of stimuli and phase in each time bin; however, for clearer visualization (since water is delivered 4 times more often than tastants; see Fig. 1*B*), the matrix rows show marginal probability distributions of phase bins for each stimulus.

Independent taste information in GC LFP and spike counts

We proceeded by estimating the MI between tastants and GC spiking activity. To that end, for each animal spike times of

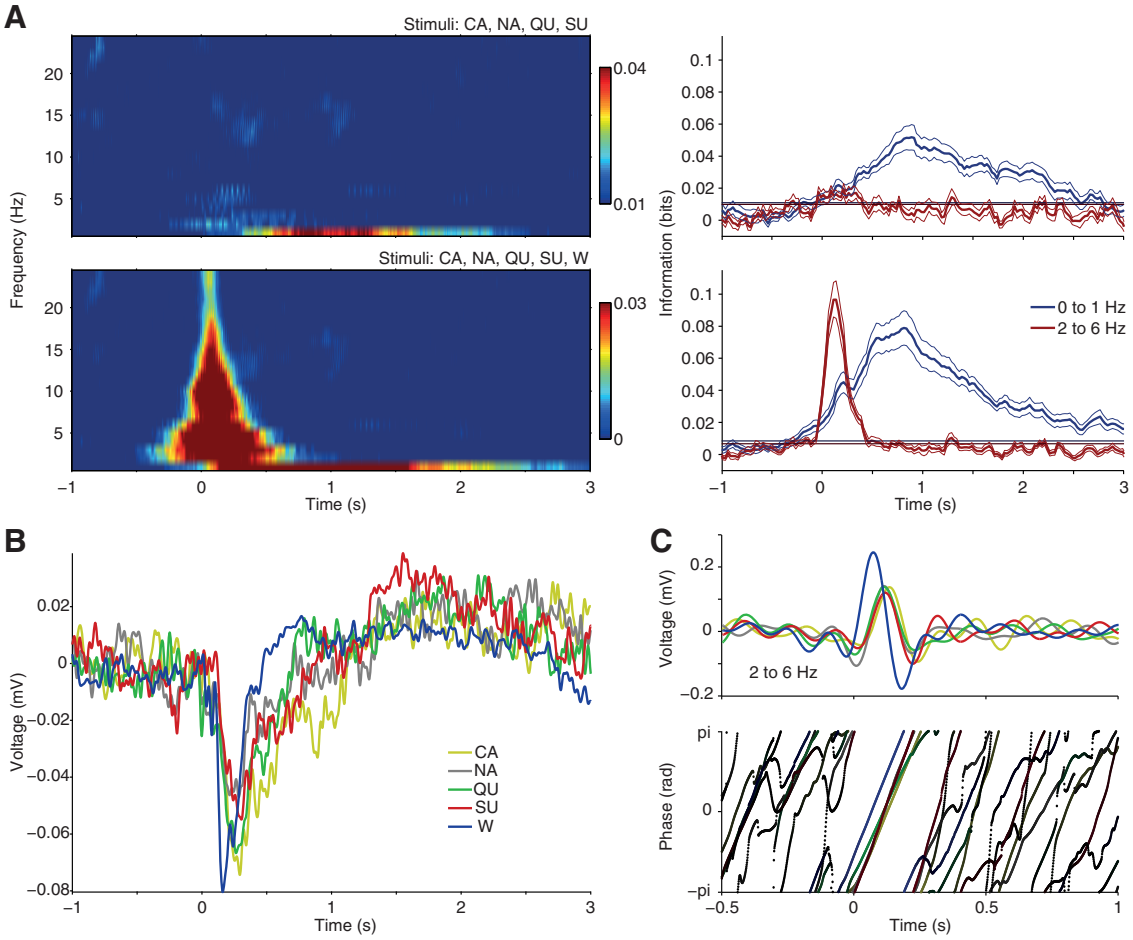

Figure 5. GC LFP phase carries information about tastants and water. ***A***, Stimulus-phase MI in low LFP frequency band (1–25 Hz), depicted as in Figure 3*A*. Higher frequency bands show no increase in information after fluid delivery (except for spurious results during opening and closure of fluid dispensers; data not shown). The time courses of the information carried by 0–1 and 2–6 Hz frequency bands are shown on the right. Note that 0–1 Hz has information about tastants from 0.5 to 2.5 s, while 2–6 Hz carries information about water from 0 to 0.5 s. Horizontal lines denote the upper limit of the 95% confidence interval of information values during baseline. ***B***, Gustatory evoked potentials (mean over rats). Notice earlier LFP deflection following water rinse compared with tastants. ***C***, Mean 2–6 Hz filtered signals (top) and mean phase series (bottom) for one exemplar LFP channel over trials. Darker dots shown on the bottom indicate low phase-reset index values.

isolated neurons were pooled and convoluted with a Gaussian function ($\sigma = 25$ ms; see Materials and Methods), generating a continuous time series of instantaneous firing rate (Fig. 7*A*,*B*). As performed to LFPs, the instantaneous firing rate of each rat was then binned into four quartiles to quantify its MI with stimuli. Figure 7*C* shows that spikes conveyed significant information about tastants, which promptly increased following fluid delivery, reached maximum value at ~1 s, and slowly decayed back to baseline levels ~4 s post stimulus. Interestingly, spike information about stimuli peaked earlier following stimulus deliver when responses to water were also taken into account. These results are explained by differences in firing rate responses to different stimuli; for example, water delivery was associated to shorter lasting spiking responses (Fig. 7*D*).

Since LFPs are believed to represent averaged synaptic activity in a local population of neurons (Logothetis, 2002), which is fomented by spikes, we next investigated whether the sensory information conveyed by LFP and spikes would be redundant, independent, or synergistic. We computed the amount of sensory information carried by spike counts and the amplitude and phase of multiple LFP frequency components at informative time intervals after taste delivery. We compared the sum of the information conveyed by the isolated analysis of amplitude, phase, or firing rate with that of the joint information of firing rate and LFP amplitude or/and phase. As shown in Figure 7*E*, the sensory information in the combined analyses of firing rate and amplitude, firing rate and phase, and firing rate and phase and amplitude was equivalent to the sum of the information carried by the corresponding marginal distributions. These results were confirmed by the same trial-shuffling procedure as applied above (data not shown). Therefore, the information carried by LFP and spike counts is not redundant but rather independent.

Discussion

We investigated the temporal dynamics of taste information conveyed by LFP and spiking activity in the GC of the awake rat. Our results show that LFP information increases from baseline levels following stimulus delivery and that the amount of information carried by different frequency components exhibits different time courses. We further obtained that the information carried by LFP amplitude and phase is independent from one another, as well as from spike information.

In agreement with our findings, recent studies showed that spikes and LFP in visual and auditory cortices of monkeys carry

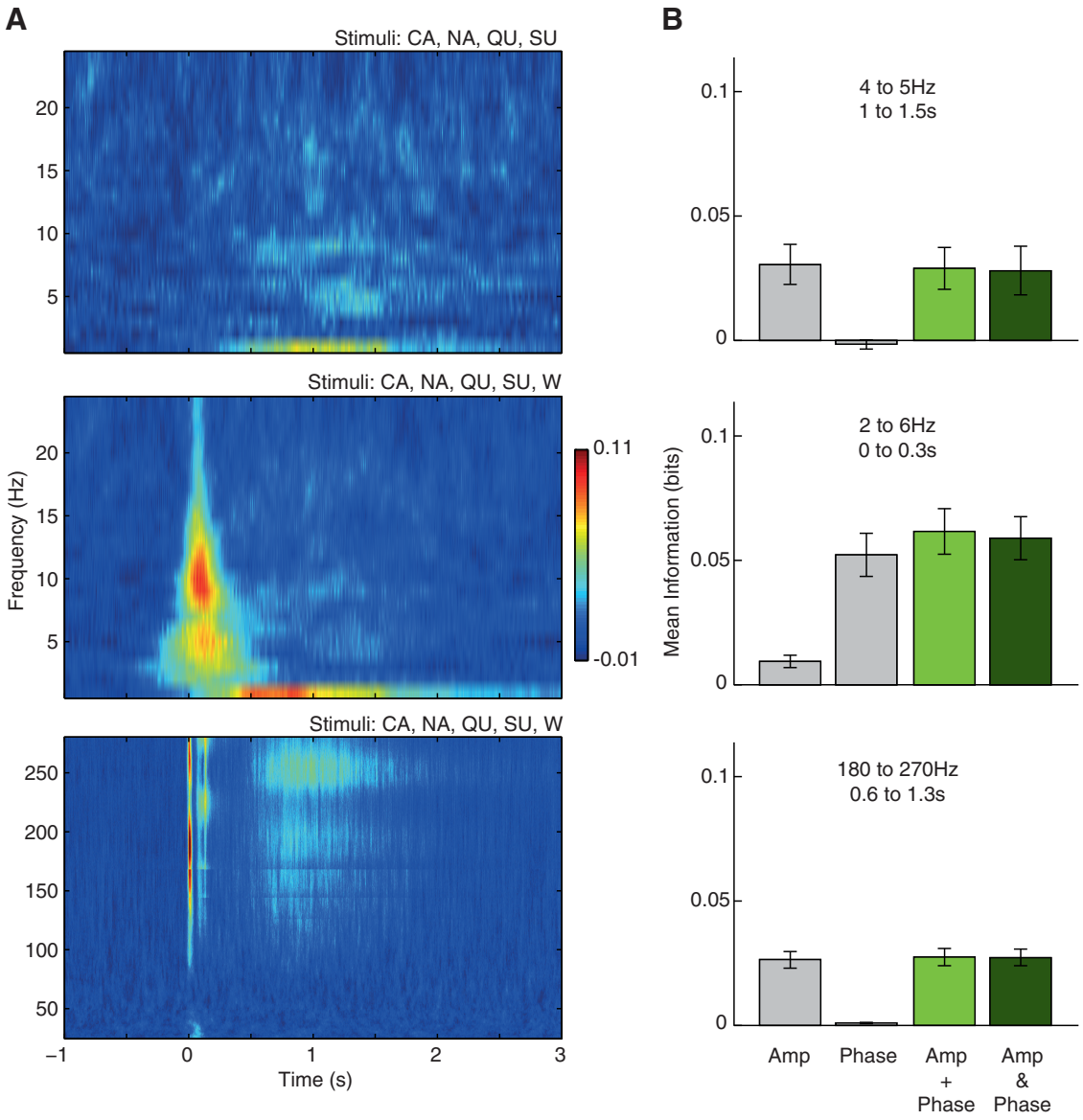

Figure 6. Gustatory information carried by LFP amplitude and phase is independent. ***A***, MI between stimuli and the joint distribution of amplitude and phase values. Notice that amplitude-phase information is high in the same frequency ranges and time intervals in which the isolated amplitude and phase information is also high (compare Figs. 3*A*, *C*, 5*A*). ***B***, Left two bars show the isolated amount of information carried by amplitude (Amp) and phase, the third bar depicts their sum, and the fourth bar shows the information carried by the joint distribution of amplitude and phase. Error bars denote SEM. Different rows show different combination of stimuli (with or without water) and analyzed LFP frequencies. Notice that the joint information is approximately the same as the sum of the isolated information values, which indicates absence of synergy or redundancy. Information may assume negative values in these analyses due to an additional bias correction to account for the different number of bins in the marginal and joint distributions (see Materials and Methods).

complementary sensory information (Belitski et al., 2008, 2010; Montemurro et al., 2008; Kayser et al., 2009). However, it should be noted that these studies differed from ours in the way the sensory stimuli were defined. Namely, monkeys were exposed to the repeated presentation of a continuous video (Belitski et al., 2008, 2010; Montemurro et al., 2008) or sound (Kayser et al., 2009; Belitski et al., 2010) in different trials. In each trial, the whole video/sound sequence was divided into nonoverlapping time windows, and each time window was defined to be a stimulus. Thus, under this framework each stimulus is a complex mixture of naturalistic features such as multiple video frames. In contrast, here we used a more standard set of stimuli: four primary tastes and water, which were delivered in isolation and spaced by 10 s. This protocol allowed us to assess information values during a baseline period, and to study the time course of information changes following stimulus delivery. Note that the dynamics of information content could not be investigated in the previous studies because time was used for defining the set of stimuli (Belitski et al., 2008, 2010; Montemurro et al., 2008; Kayser et al., 2009). In addition, here we have identified stimulus-specific changes in the amplitude and phase of LFP components that account for the high information values. For example, we observed that the amplitude of high-frequency LFP components following stimulus delivery was different for the different tastes, with CA associated with the highest amplitude (Fig. 3*D*). Similarly, we observed that the phase reset of low-frequency GC LFP oscillations (Tort et al., 2010) is advanced following water delivery on the tongue (Fig. 5*C*).

Our analysis showed that the phase of 2–15 Hz LFP components are not informative about the basic tastants (Fig. 5*A*), since

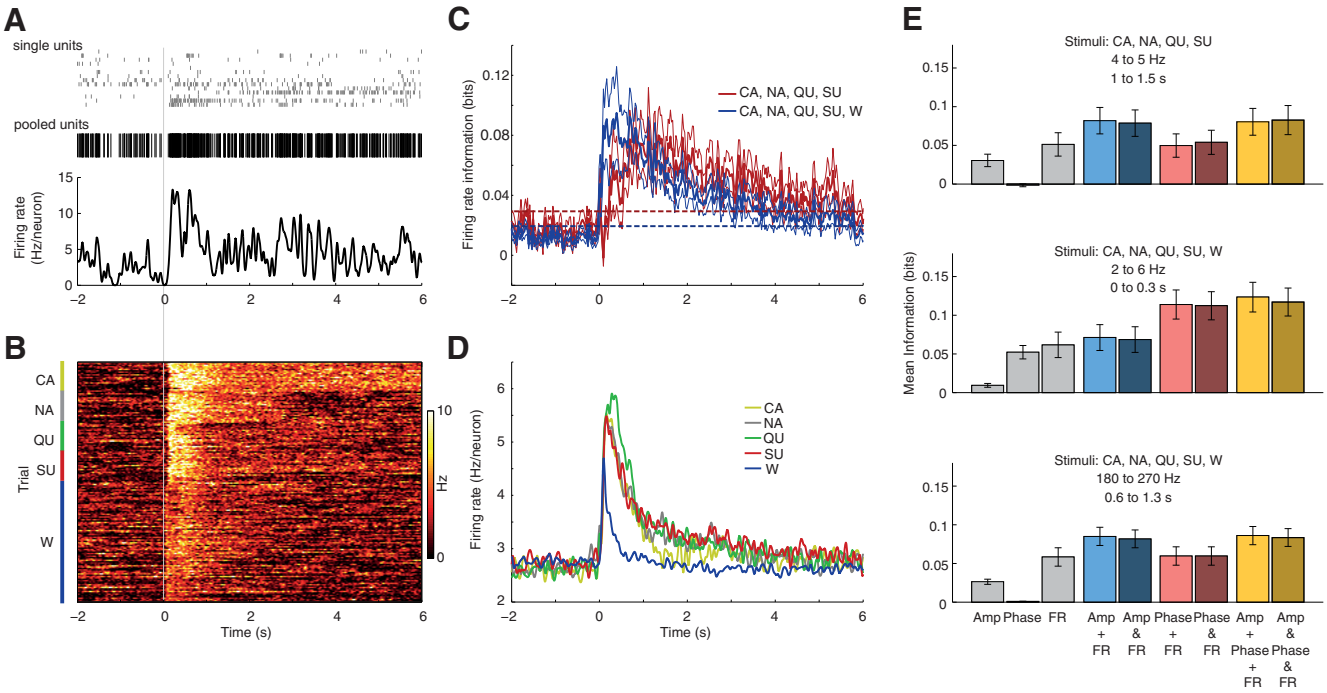

Figure 7. LFP and spike information are independent. ***A***, Tastant information in pooled neuronal firing rate. Top, Spiking activity of nine neurons during an example trial, along with the pooled unit activity. Bottom, Mean firing rate; the time series of continuous firing rate is obtained by convolving pooled spike times with a Gaussian ($\sigma = 25$ ms). ***B***, Pooled firing rate for all trials of each stimulus for a representative animal. ***C***, Tastant and tastant plus water information carried by pooled spiking activity (mean $\pm$ SEM over rats). Notice that the inclusion of water as a stimulus leads to an earlier increase of MI. Dashed lines denote the upper limit of the 95% confidence interval of information values during baseline. ***D***, Mean firing rate for the five fluids; notice that water induces the shortest response. ***E***, As in Figure 6*B*, but for the isolated and joint distributions of amplitude (Amp), phase, and firing rate (FR). Notice absence of synergy or redundancy among the information carried by spiking activity and LFP amplitude and phase.

all of them induce an identical pattern of oscillatory reset, as seen by band-filtered evoked potentials (Fig. 5*C*). Curiously, however, by considering different time bins as representing different stimuli as in previous work (Belitski et al., 2008, 2010; Montemurro et al., 2008; Kayser et al., 2009), we found that the instantaneous LFP phase becomes highly informative (data not shown). This is explained by the fact that different time bins are associated with specific phases due to the duration of the evoked potential/oscillatory reset that outlasts the period of sensory stimulation (Picton and Hillyard, 1974; Courchesne et al., 1975; Tort et al., 2010; Privman et al., 2011). Thus, while the oscillatory reset is likely related to the processing of the sensory stimulus, we note that under this analytical framework the information carried by LFP phase is not about the stimulus itself but about time. In this sense, given that visual and auditory stimuli may induce oscillatory resets, it would be interesting to know whether the amount of information carried by LFP phase and amplitude reported in previous studies (Belitski et al., 2008, 2010; Montemurro et al., 2008; Kayser et al., 2009) would change by randomizing the order of visual or auditory stimuli; for example, it may have been the case that the oscillatory reset induced by a given stimulus A would have influenced LFP phase during the subsequent presentation of a stimulus B that by itself would cause no LFP response. In the present work, we used large interstimulus intervals and randomized stimulus presentation; under this protocol, we were able to demonstrate that GC LFPs carry sensory information.

Spiking activity exhibited high information about tastants, peaking at ~1 s after peripheral stimulation with basic tastants, and ~400 ms when water was taken into account (which is readily explained by the shorter transient of spike responses to water; Fig. 7*D*). To our knowledge, this is the first description of the dynamics of taste information in the instantaneous spike rate of a population of GC neurons. Similar analyses have been previously reported for the instantaneous firing rate of individual neurons in the geniculate ganglion, which carried taste information with comparable time courses (Lawhern et al., 2011). In the somatosensory system, it has been shown that the cumulative information–the amount of information as a function of the time length from stimulus onset used for counting spikes–reaches steady values >50 ms (Panzeri et al., 2001; Petersen et al., 2001; Arabzadeh et al., 2004, 2006). Consistent with this, using a similar sliding window approach as ours, Arabzadeh et al. (2004, 2006) showed that the "ongoing information" about whisker vibration in spikes from the barrel cortex and trigeminal ganglion increases immediately after simulation and decreases 150 ms afterward. Notice that the information time course about vibrissae movements in spikes substantially differs from the time course of tastant information reported here, which could last up to 4–5 s after peripheral stimulation (Fig. 7*C*). This result indicates that taste coding is complex, and likely involves palatability representations that must integrate information from multiple brain regions (Katz et al., 2002; Jones et al., 2006; Piette et al., 2012).

Mounting evidence suggests that high-frequency LFP components (>100 Hz) represent spectral leakage from extracellular spikes, and that their instantaneous amplitude would constitute a proxy for tracking multi-unit activity (Jia and Kohn, 2011, Belluscio et al., 2012; Ray and Maunsell, 2011; Telenczuk et al., 2011). However, it has recently been demonstrated that this is not

always the case, and that whether the highest frequency range of the LFP spectrum is contaminated by spiking activity or not should be examined on an individual basis (Scheffer-Teixeira et al., 2013). In the present work, we found that both LFP components >100 Hz and population spike counts dynamically represent taste information (Figs. 3*C*, 7*C*), which indicates that these two signals might be related. However, taste information in spike counts and in LFP frequencies >100 Hz exhibited different time courses, with the former being considerably longer. In addition, the time course of tastant information in spike counts, but not in LFP components >100 Hz, depended on whether water was considered as a stimulus (compare Figs. 3*C*, left, 7*C*). Furthermore, these signals showed different response magnitudes for the different tastants; for example, CA was associated with the highest LFP amplitude at 180–270 Hz, which was not the case for spike counts (compare Figs. 3*B*, 7*D*). Finally, synergy analyses showed that both signals are rather independent, since the information carried by their joint probability is not different from the sum of the information carried by each signal individually (Fig. 7*E*, bottom). In all, these results suggest that spike counts and high-frequency LFP components code for different features of the stimulus.

The nonredundancy between the amplitude and phase of LFPs and spiking activity observed here is generally consistent with previous findings. Namely, Montemurro et al. (2008) and Belitski et al. (2008) reported that the information in LFP and spiking activity in the primary visual cortex of monkeys is not redundant, while Kayser et al. (2009) obtained similar results in recordings from the monkey auditory cortex. In addition, Kayser et al. (2009) also showed that the joint information in amplitude and phase is higher than their individual information; unfortunately, specific measures of synergy/redundancy were not computed in this study. Upon visual inspection of their Figure 1*C*, it seems that the joint distribution may actually carry more information than the sum of the information in the marginal distributions, suggesting synergy. However, it should be noted that here we have controlled for the bias introduced by the different number of bins in the individual (4 bins) in joint distributions (e.g., $4 \times 4 = 16$ bins) by subtracting information values during the baseline period, which is a different procedure from Kayser et al. (2009). In addition, we obtained the same results of information independence when performing a new set of analyses that relied on computing joint distributions after shuffling trials within the same stimulus, thus preserving marginal distributions (Schneidman et al., 2003). Nevertheless, whether peripheral information may be independent and complementary in some sensory cortex (as the GC) while synergistic in others (as the auditory cortex) remains to be demonstrated under a similar experimental protocol and analytical framework.

In summary, we have examined taste coding in GC by assessing the dynamics of information content in LFP signals following sensory stimulation. We found significant increases in information values from baseline levels in the phase and amplitude of multiple LFP bands, which were nonredundant and complementary to spiking activity. These results provide new insights into the time course of physical and hedonic representation of tastes (Katz et al., 2001, 2002).

References

Arabzadeh E, Panzeri S, Diamond ME (2004) Whisker vibration information carried by rat barrel cortex neurons. J Neurosci 24:6011–6020. CrossRef Medline

Arabzadeh E, Panzeri S, Diamond ME (2006) Deciphering the spike train of a sensory neuron: counts and temporal patterns in the rat whisker pathway. J Neurosci 26:9216–9226. CrossRef Medline

Belitski A, Gretton A, Magri C, Murayama Y, Montemurro MA, Logothetis NK, Panzeri S (2008) Low-frequency local field potentials and spikes in primary visual cortex convey independent visual information. J Neurosci 28:5696–5709. CrossRef Medline

Belitski A, Panzeri S, Magri C, Logothetis NK, Kayser C (2010) Sensory information in local field potentials and spikes from visual and auditory cortices: time scales and frequency bands. J Comput Neurosci 29:533–545. CrossRef Medline

Belluscio MA, Mizuseki K, Schmidt R, Kempter R, Buzsáki G (2012) Cross-frequency phase-phase coupling between θ and γ oscillations in the hippocampus. J Neurosci 32:423–435. CrossRef Medline

Courchesne E, Hillyard SA, Galambos R (1975) Stimulus novelty, task relevance and the visual evoked potential in man. Electroencephalogr Clin Neurophysiol 39:131–143. CrossRef Medline

Delorme A, Makeig S (2004) EEGLAB: an open source toolbox for analysis of single-trial EEG dynamics including independent component analysis. J Neurosci Methods 134:9–21. CrossRef Medline

Jia X, Kohn A (2011) Gamma rhythms in the brain. PLoS Biol 9:e1001045. CrossRef Medline

Jones LM, Fontanini A, Katz DB (2006) Gustatory processing: a dynamic systems approach. Curr Opin Neurobiol 16:420–428. CrossRef Medline

Katz DB, Simon SA, Nicolelis MA (2001) Dynamic and multimodal responses of gustatory cortical neurons in awake rats. J Neurosci 21:4478–4489. Medline

Katz DB, Nicolelis MA, Simon SA (2002) Gustatory processing is dynamic and distributed. Curr Opin Neurobiol 12:448–454. CrossRef Medline

Kayser C, Montemurro MA, Logothetis NK, Panzeri S (2009) Spike-phase coding boosts and stabilizes information carried by spatial and temporal spike patterns. Neuron 61:597–608. CrossRef Medline

Lawhern V, Nikonov AA, Wu W, Contreras RJ (2011) Spike rate and spike timing contributions to coding taste quality information in rat periphery. Front Integr Neurosci 5:18. CrossRef Medline

Lemon CH, Smith DV (2006) Influence of response variability on the coding performance of central gustatory neurons. J Neurosci 26:7433–7443. CrossRef Medline

Logothetis NK (2002) The neural basis of the blood-oxygen-level-dependent functional magnetic resonance imaging signal. Philos Trans R Soc Lond B Biol Sci 357:1003–1037. CrossRef Medline

Magri C, Whittingstall K, Singh V, Logothetis NK, Panzeri S (2009) A toolbox for the fast information analysis of multiple-site LFP, EEG and spike train recordings. BMC Neurosci 10:81. CrossRef Medline

Montemurro MA, Rasch MJ, Murayama Y, Logothetis NK, Panzeri S (2008) Phase-of-firing coding of natural visual stimuli in primary visual cortex. Curr Biol 18:375–380. CrossRef Medline

Nicolelis MA, Ghazanfar AA, Faggin BM, Votaw S, Oliveira LM (1997) Reconstructing the engram: simultaneous, multisite, many single neuron recordings. Neuron 18:529–537. CrossRef Medline

Panzeri S, Treves A (1996) Analytical estimates of limited sampling biases in different information measures. Network 7:87–107. CrossRef

Panzeri S, Petersen RS, Schultz SR, Lebedev M, Diamond ME (2001) The role of spike timing in the coding of stimulus location in rat somatosensory cortex. Neuron 29:769–777. CrossRef Medline

Panzeri S, Senatore R, Montemurro MA, Petersen RS (2007) Correcting for the sampling bias problem in spike train information measures. J Neurophysiol 98:1064–1072. CrossRef Medline

Petersen RS, Panzeri S, Diamond ME (2001) Population coding of stimulus location in rat somatosensory cortex. Neuron 32:503–514. CrossRef Medline

Picton TW, Hillyard SA (1974) Human auditory evoked potentials. II: effects of attention. Electroencephalogr Clin Neurophysiol 36:191–199. CrossRef Medline

Piette CE, Baez-Santiago MA, Reid EE, Katz DB, Moran A (2012) Inactivation of basolateral amygdala specifically eliminates palatability-related information in cortical sensory responses. J Neurosci 32:9981–9991. CrossRef Medline

Privman E, Fisch L, Neufeld MY, Kramer U, Kipervasser S, Andelman F, Yeshurun Y, Fried I, Malach R (2011) Antagonistic relationship between gamma power and visual evoked potentials revealed in human visual cortex. Cereb Cortex 21:616–624. CrossRef Medline

Ray S, Maunsell JH (2011) Different origins of gamma rhythm and high-gamma activity in macaque visual cortex. PLoS Biol 9:e1000610. CrossRef Medline

Sadacca BF, Rothwax JT, Katz DB (2012) Sodium concentration coding gives way to evaluative coding in cortex and amygdala. J Neurosci 32: 9999–10011. CrossRef Medline

Samuelsen CL, Gardner MP, Fontanini A (2012) Effects of cue-triggered expectation on cortical processing of taste. Neuron 74:410–422. CrossRef Medline

Scalera G (2000) Taste preference and acceptance in thirsty and dehydrated rats. Physiol Behav 71:457–468. CrossRef Medline

Scheffer-Teixeira R, Belchior H, Leão RN, Ribeiro S, Tort AB (2013) On high-frequency field oscillations (>100 Hz) and the spectral leakage of spiking activity. J Neurosci 33:1535–1539. CrossRef Medline

Schneidman E, Bialek W, Berry MJ 2nd (2003) Synergy, redundancy, and independence in population codes. J Neurosci 23:11539–11553. Medline

Telenczuk B, Baker SN, Herz AV, Curio G (2011) High-frequency EEG covaries with spike burst patterns detected in cortical neurons. J Neurophysiol 105:2951–2959. CrossRef Medline

Tort AB, Fontanini A, Kramer MA, Jones-Lush LM, Kopell NJ, Katz DB (2010) Cortical networks produce three distinct 7–12 Hz rhythms during single sensory responses in the awake rat. J Neurosci 30:4315–4324. CrossRef Medline

Yamamoto T, Matsuo R, Kiyomitsu Y, Kitamura R (1989) Taste responses of cortical neurons in freely ingesting rats. J Neurophysiol 61:1244–1258. Medline